Preferred citation: C. Fellers, B. Westerlind and A. de Ruvo. An investigation of the biaxial failure envelope of paper: experimental study and theoretical analysis. In **The role of fundamental research in paper-making**, *Trans. of the VIIth Fund. Res. Symp. Cambridge, 1981*, (Fundamental Research Committee, ed.), pp 527–559, FRC, Manchester, 2018. DOI: 10.15376/frc.1981.1.527.

AN INVESTIGATION OF THE BIAXIAL FAILURE ENVELOPE OF PAPER: EXPERIMENTAL STUDY AND THEORETICAL ANALYSIS

Christer Fellers, Bo Westerlind and Alf de Ruvo,
Swedish Forest Products Research Laboratory,
Box 5604,
S-114 86 Stockholm,
Sweden.

Abstract

In the theoretical part of this paper, the Tsai-Wu tensor theory is used to determine the equation for the biaxial strength envelope of a material.

One great advantage of using the Tsai-Wu theory for investigating biaxial strength envelopes is that it may be transformed to arbitrary co-ordinate axes by means of tensor transformation laws.

In the experimental part of the paper, the strengths in compression and shear are evaluated using thick-walled tubes consisting of two layers of paper glued together with a non-penetrating glue. In addition, the strength of paper under biaxial stress is determined by subjecting paper tubes to axial tension or compression combined with a radial tension caused by internal pressure.

In the final part of the paper, the application of the Tsai-Wu tensor theory to the prediction of failure of a corrugated container is discussed, as well as practical means of limiting the number of experiments necessary to establish the biaxial failure envelope of paper.

Introduction

In practice, paper as a packaging material usually fails under biaxial loading, whether in the case of a filled paper sack's being dropped or in the case of the failure of a corrugated container subjected to internal pressure and external loading.

The top-to-bottom compression strength of corrugated containers has been a property of interest to the packaging industry for a long time. Early investigations in this area were reviewed by McKee, Gander and Wachuta(1), who also did extensive work on the subject. It was assumed that the corrugated board at the vertical edges fails at a stress level which is related to its edgewise compression strength as evaluated by short column compression tests. The important material properties for the ultimate load-bearing ability of a container were, in the early investigations, approached by semi-empirical means. The reason was that the box in the post-buckling range presented difficulties for theoretical analysis.

More recently a different approach has been taken by Peterson and Fox(2-4) towards understanding container performance. The corrugated board is treated as an engineering structure and the stress distribution in the liners, due to the compression and bending, is analysed with conventional methods of engineering mechanics and structural analysis.

Since it is recognised that the failure of a container is always compressive in nature, the critical side of the corrugated board is considered in their analysis to be the concave side, usually the inside. As a result of their analysis the biaxial principal stress distribution on the surface of the panel was calculated with regard to both magnitude and direction. Biaxial strength values for liner-board were, however, not available for their failure prediction analysis and a simplified method had to be used.

In the present work the aim is to:

1. Discuss several biaxial strength theories from the viewpoint of their application to paper.

2. Establish the general shape of the biaxial failure envelope of paper by the use of two-layer tubular specimens bonded together by an adhesive.

3. Discuss possible simplifications of testing conditions to obtain a practical way of establishing the parameters in the Tsai-Wu criterion for paper.

4. Discuss the application of the Tsai-Wu tensor theory to the failure characteristics of a corrugated container.

General Background

At present one of the most common paper strength tests used in the paper industry is the uniaxial tensile test. Recently, reliable uniaxial compression tests have also been developed[5,6]. Apart from the familiar burst test[7], which may be characterised as an uncontrolled biaxial tensile test, few investigations on the biaxial strength properties of paper have been reported :

Biaxial shear-tensile loading and uniaxial compression loading was used by Setterholm et al.[8,9] on tubular paper specimens. Flat specimens subjected to biaxial tensile loading were used by Uesaka et al.[10], primarily for stress-strain investigations prior to failure.

Tubular specimens subjected to axial loading, combined with internal pressure, were used by de Ruvo, Carlsson, and Fellers[11] in the determination of the failure envelope of kraft paper and sack paper in the biaxial tensile mode.

Several theories for yielding and failure in materials under combined stresses have been proposed[12-17]. The aim of these theories is to define a function of all stress components that reaches a critical value for different combinations of stress. This function is called the yield or failure criterion.

Paper may be described as an orthotropic laminate[18], and it is important to emphasise an important distinction between the yield or failure criterion for isotropic and that for orthotropic materials[19].

Any biaxial stress state in an isotropic material may be expressed by two principal stresses (σ_1 and σ_2). The resulting yield or failure criterion then corresponds to a two-dimensional figure such as figure 1, which illustrates the two main theories for defining failure by yielding. the Tresca criterion (maximum shear theory) and the Huber-von Mises criterion (distortion energy theory)[20]. In this figure, the first quadrant represents biaxial tensile strength, the second and fourth represent biaxial tension and compression strength, and the third biaxial compression strength.

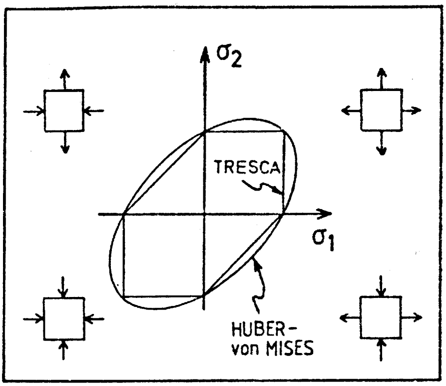

Fig 1—The Tresca and Huber-von Mises yield criteria for isotropic materials under biaxial stress.

When the yield or failure criterion for an orthotropic material such as paper is considered, the stresses are preferably related to the principal axes of material symmetry, MD and CD. For a biaxial stress state, this means that, in addition to the normal stresses σ_x, σ_y the shear stress σ_s must also be considered. This means that there are three stress components in the criterion.

Theoretical Considerations - The Tsai-Wu Tensor Theory

Failure in composite materials involves many modes, such as fibre failure, matrix failure, interfacial failure, delamination, and buckling. The various modes interact and can occur concurrently and sequentially. In general, therefore, strength criteria for anisotropic materials such as composites and paper are not intended to explain the mechanisms of failure.

In any phenomenological failure criterion, the shape of the failure envelope is never completely known until experiments are performed for all possible combined states of stress. Nevertheless, the degree of accuracy of a failure envelope has to be a compromise between engineering requirements and availability of effort and time.

Tsai and Wu[14-16] introduced a failure criterion for anisotropic materials which offers a significant improvement in operational simplicity over many current failure criteria. This theory has previously been used to predict the failure envelope of paper in biaxial tension[11], and is also used in the present investigation. The basic assumption is that there exists a failure surface in the stress space of the following form.

$$F_i \cdot \sigma_i + F_{ij} \cdot \sigma_i \cdot \sigma_j = 1 \tag{1}$$

where F_i and F_{ij} are strength tensors, σ_i and σ_j are stresses, and i, j = 1, 2, ..., 6.

1. Two-dimensional case - anisotropic materials

Expanding equation (1) for the two-dimensional state of stress, i,j = 1,2,6, we obtain the equation of the failure surface in a quadratic form.

$$\begin{aligned} &F_{11} \cdot \sigma_1^2 + F_{22} \cdot \sigma_2^2 + F_{66} \cdot \sigma_6^2 + 2F_{12} \cdot \sigma_1 \cdot \sigma_2 + 2F_{16} \cdot \sigma_1 \cdot \sigma_6 \\ &+ 2F_{26} \cdot \sigma_2 \cdot \sigma_6 + F_1 \cdot \sigma_1 + F_2 \cdot \sigma_2 + F_6 \cdot \sigma_6 = 1 \end{aligned} \tag{2}$$

In the two-dimensional state of stress the failure surface is three-dimensional, see Fig. 2, since there are three independent stress components σ_1, σ_2, and σ_6, two normal and one shear.

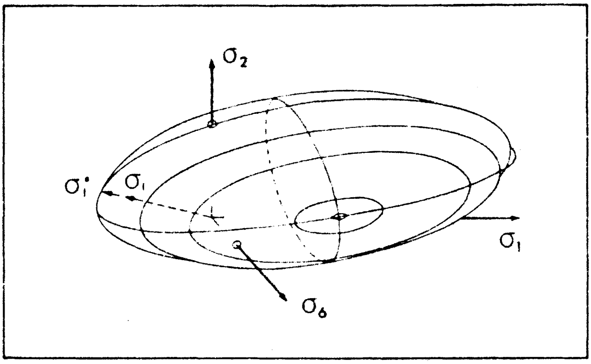

Fig 2—A two-dimensional state of stress may be visualized as a three-dimensional ellipsoid. σ_1 and σ_2 are the normal stresses, σ_6 is the shear stress.

2. Two-dimensional case - Orthotropic materials

on axis \ off axis	σ_1	σ_2	
σ_x	m^2	n^2	$2mn$
σ_y	n^2	m^2	$-2mn$
σ_s	$-mn$	mn	$m^2 - n^2$

$m = \cos\theta \quad n = \sin\theta$

Table 1

Transformation of stress components due to co-ordinate rotation, from off- to on-axis. (Fig.3 defines angles.)

In engineering analyses, the co-ordinate axes are usually chosen with respect to the structure so as to simplify the boundary conditions. In research work it is essential to be able to distinguish between the influences of compressive, tensile, and shear stresses on the biaxial strength behaviour, and it is preferable to relate the stresses to the principal axes of symmetry of the orthotropic material. In the case of paper the natural co-ordinate system is made up of its orthotropic axes, i.e. when the 1-axis coincides with the machine direction (MD) and the 2-axis with the cross machine direction (CD). This co-ordinate system is called on-axis. Any plane off-axis stress state may be transformed on-axis by means of Table 1, where the on-axis stresses have subscripts x, y, and s and off-axis stresses have subscripts 1, 2, and 6. Note that the co-ordinate rotation for all stress transformations is counter-clockwise from off-axis to on-axis, as illustrated in figure 3.

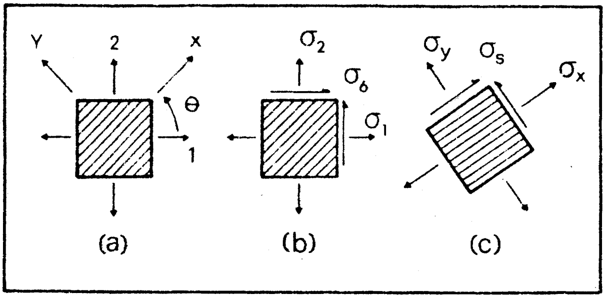

Fig 3— (a) Relation between the 1—2 and x—y systems. Counterclockwise rotation is positive. (b) The off-axis stress components, with numerical subscripts. (All stresses are shown positive.) (c) The on-axis stress components, with literal subscripts. (All stresses are shown positive.)

Sign reversal for the normal stress components, from tensile to compressive, is known to have significant effect on the strength of paper, but when the material is loaded in its orthotropic directions the strength should be unaffected by the sign of the shear stress component σ_s. Thus all those terms in Equation (2) which contain linear or first degree shear stress are zero and may be deleted from the equation.

For orthotropic materials we then obtain equation (3):

$$F_{xx}.\sigma_x^2 + 2.F_{xy}.\sigma_x.\sigma_y + F_{yy}.\sigma_y^2 + F_{ss}.\sigma_s^2 + F_x.\sigma_x + F_y.\sigma_y = 1 \qquad (3)$$

The three dimensional failure surface shown in Figure 2 may be projected onto the normal stress plane, as illustrated for on-axis loading in Figure 4, where each ellipse represents a constant positive or negative shear stress.

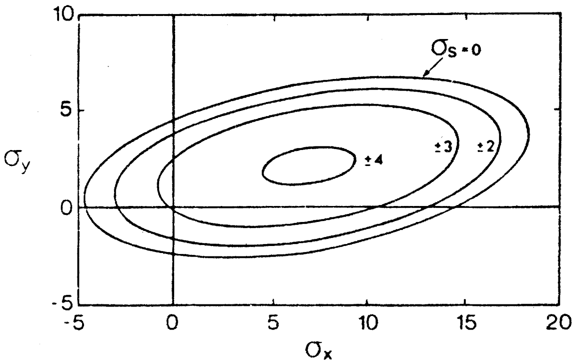

Fig 4—The three-dimensional ellipsoid in Fig 2 projected on the $\sigma_x - \sigma_y$ plane. For on-axis loading each ellipse represents both positive and negative shear.

There are four quadratic and two linear strength parameters in equation (3). In order to determine the six of them certain key tests are carried out. They represent the minimum number of measurements necessary to describe the failure stress space of the material.

Of the key parameters whose values are needed, five are illustrated in Figure 5, where

X = MD tensile strength
X′= MD compressive strength
Y = CD tensile strength
Y′= CD compressive strength
and P = biaxial strength

In addition, the shear strength S must be evaluated.

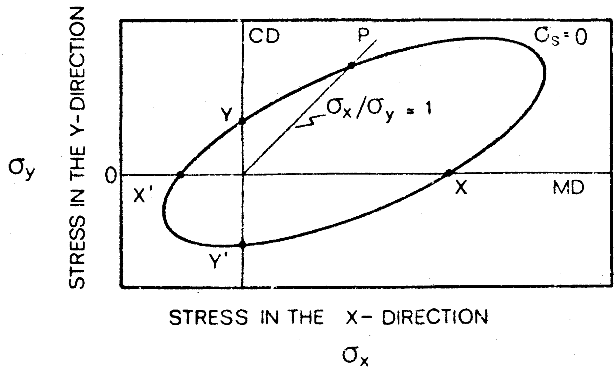

Fig 5—The shape of the failure envelope in the $\sigma_x-\sigma_y$ ($\sigma_s = 0$) plane must be determined from one biaxial and four uniaxial measurements.
X = MD tensile strength, X′ = MD compression strength
Y = CD tensile strength, Y′ = CD compression strength
P = biaxial strength.

The derivations of the relations between the constants in Equation (3) and the engineering strength values determined by the key tests are given below.

Determination of F_{xx}, F_x, F_{yy} and F_y

The measured MD and CD strength values in tension and compression are substituted into equation (3), which yields:

$$F_{xx} = 1/XX' \tag{4}$$
$$F_x = 1/X - 1/X' \tag{5}$$
$$F_{yy} = 1/YY' \tag{6}$$
$$F_y = 1/Y - 1/Y' \tag{7}$$

Determination of F_{xy}

The term F_{xy} is related to the interaction between the two normal stress components. This coefficient can only be measured if both normal stress components are non-zero. This requires a biaxial test.

The strength component F_{xy} can be determined by an infinite number of stress combinations(15,21). As shown in figure 5, one simple yet reliable way of determining F_{xy} is to impose equal biaxial tensions such as

$$\sigma_x = \sigma_y = P \ , \ \sigma_s = 0$$

Substituting this stress combination into equation (3), we obtain.

$$F_{xy} = \frac{1}{2P^2}\left[1 - P\left(\frac{1}{X} - \frac{1}{X'} + \frac{1}{Y} - \frac{1}{Y'}\right) - P^2\left(\frac{1}{XX'} + \frac{1}{YY'}\right)\right] \tag{8}$$

Tsai and Hahn(17) introduce a dimensionless interaction coefficient

$$F^*_{xy} = F_{xy} \Big/ \sqrt{F_{xx} \cdot F_{yy}} \tag{9}$$

Assuming that the orthotropic failure criterion given by equation (3) is a generalisation of the von Mises criterion, F^*_{xy} adopts a constant value.

$$F^*_{xy} = -0.5 \tag{10}$$

Determination of F_{ss}

The shear strength S is determined in a separate experiment. Substituting the shear strength S into equation (3) for $\sigma_x = \sigma_y = 0$, we obtain.

$$F_{ss} = 1/S^2 \tag{11}$$

3. Transformations in the stress space

The tensor form of equation (3) enables the stresses obtained along the principal material directions to be transformed to any reference directions.

The transformations of the quadratic and linear parameters are listed in Table 2.

on axis / off axis	F_{xx}	F_{yy}	F_{xy}	F_{ss}
F_{11}	m^4	n^4	$2m^2n^2$	m^2n^2
F_{22}	n^4	m^4	$2m^2n^2$	m^2n^2
F_{12}	m^2m^2	m^2n^2	m^4+n^4	$-m^2n^2$
F_{66}	$4m^2n^2$	$4m^2n^2$	$-8m^2n^2$	$(m^2-n^2)^2$
F_{16}	$2m^3n$	$-2mn^3$	$2(m^3n-mn^3)$	mn^3-m^3n
F_{26}	$2mn^3$	$-2m^3n$	$2(m^3n-mn^3)$	m^3n-mn^3

$m = \cos\theta \quad n = \sin\theta$

on axis / off axis	F_x	F_y
F_1	m^2	n^2
F_2	n^2	m^2
F_6	$2mn$	$-2mn$

where $m = \cos\theta$ and $n = \sin\theta$

Table 2

Transformation of quadratic and linear strength parameters in stress space in power functions from on axis to off axis. (See figure 3 for definitions of angles.)

4. Safety Factor

The failure criterion such as that in equation (2) or (3) specifies the conditions of failure.

$$f(\sigma_1, \sigma_2, \sigma_6) = 1 \qquad (12)$$

The severity of the imposed stress state may be expressed by the strength ratio R which indicates the quantitative measure-of-safety margin(7), defined according to

$$R = \sigma_i / \sigma_i^* \qquad (13)$$

where σ_i^* is the allowable stress vector satisfying equation (12) and σ_i is the imposed stress vector.

Instead of solving for the failure criterion, we now solve for the strength ratio.

$$\left[F_{ij} \cdot \sigma_i \cdot \sigma_j\right] R^{-2} + \left[F_i \cdot \sigma_i\right] R^{-1} = 1 \qquad (14)$$

There are two roots of R corresponding to stress vectors in opposite directions. Only the positive root has physical meaning. The physical meaning of R is the ratio of vectors R_i / R_i^* in figure 2. (The negative root corresponds to the strength ratio obtained for an imposed stress $(-\sigma_i)$).

To summarise.

- When the applied stress is zero, R = 0)
- When the stress is safe, $R < 1$
- Failure occurs when R = 1

Experimental Considerations

1. Test material

The testing material for this investigation was a commercial liner-board of substance 125 g/m^2 with a thickness of 0.21 mm.

2. Tubular specimen preparation and loading

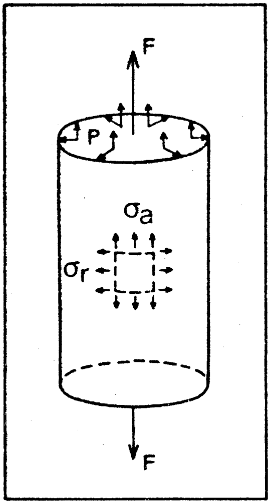

Fig 6—The tube may be exposed to combinations of axial-radial loading by applying axial tensile or compressive loads and internal pressure.

For this type of biaxial testing, the use of thin-walled tubular specimens constitutes the most standard procedure available(22).

As illustrated in figure 6, any desired state of plane stress in the axial and radial directions may be obtained if the tube is simultaneously subjected to an axial force and an internal pressure in a pre-selected ratio. Furthermore, a shear component may be superimposed by rotating the tube in torsion.

However, in this investigation shear stress was obtained by applying a biaxial compression tension loading on a 45^{o} specimen.

For an isotropic material, the buckling load of a cylinder is found to be proportional to t/D, where t is the paper thickness and D is the cylinder diameter(23). To obtain maximum stability by increasing the thickness it was decided to manufacture a two-layer paper tube where the paper-layers were glued together. Information on adhesive selection, specimen preparation and loading is given below. A two-layer tube offers the advantage that both layers may be exposed to the controlled humidity environment for a sufficient time prior to testing. Maximum stability is achieved when the diameter D is as small as possible, but the strain gradient introduced in the paper in the thickness direction on bending into a tube sets a lower limit to D.

As a compromise between the demands of stability and the avoidance of residual stresses, tubes of diameter 40 mm and length 100 mm were used in this study. The maximum strain e in the surface layers is a function of thickness t and diameter D, through the following expression[20]:

$$e = t/D$$

This means that the maximum strain for each of the layers is about 0.5%.

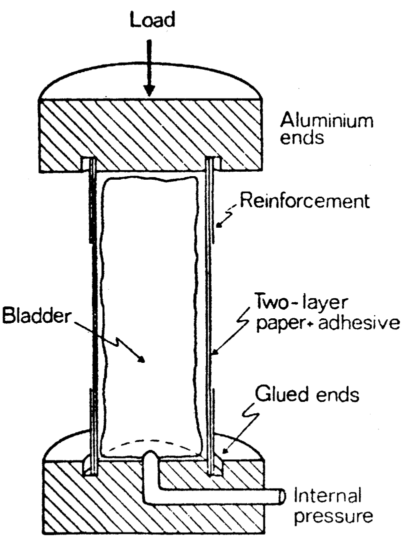

Fig 7—Principle of construction of the two-layer tubular specimen.

In a previous study[24] it was shown that paper board subjected to bending is governed by compressive stress-strain behaviour[24] and that failure in bending occurs at a compressive strain in the concave part of the board of about twice that obtained in pure compression. Considering that the strain-to-failure in pure compression is about 0.5%, as shown in Table 3, the chosen 40 mm diameter tubes should have a satisfactory safety factor against premature failure due to bending.

For biaxial tensile tests, single layer, 80 mm diameter tubes were also used.

Experiments in the biaxial compression mode are the most difficult to perform. They require the application of external pressure to the tube. To the authors´ knowledge no other techniques for obtaining data in the third quadrant for thin laminates or similar materials have been reported in the literature.

The construction of a two-layer tube is shown in figure 7.

The sequence for preparing and testing a tubular specimen involves the following steps:

1. Cutting the flat specimen to size.
2. Application of adhesive.
3. Wrapping of sample on cylinder.
4. Attaching reinforcing end tabs.
5. Achieving equilibrium moisture conditions.
6. Gluing the tube to aluminium ends.
7. Application of a combination of axial and radial loads

A specimen is taken from a flat sheet and rolled into a tube on a mandrel of diameter equal to the inner aluminium end. In order to produce as perfect tubes as possible a special apparatus has been constructed. The paper is fastened to the cylindrical mandrel by adhesive tape and rolled almost one turn. A rubbery adhesive is then applied to the remainder of the paper by a wire-wound roller drawn parallel to the tube axis on a flat table to ensure a uniform dry adhesive layer of 35 g/m^2 weight. The mandrel is then turned until the paper has been wrapped twice round it with an additional overlap of 5 mm. The overlap is glued with epoxy glue.

In order to obtain a good bond between the two paper layers and a close fit to the mandrel, the paper is pressed with a line pressure of 10 N/cm to the mandrel.

The specimen´s ends are reinforced against crushing to ensure failure in the middle of the tube. To do this a third layer of paper, 25 mm long, is glued to each tube end.

After the adhesives have cured sufficiently to permit handling, the tube ends are clean cut parallel and the tubes are put aside for one week to allow the adhesive to dry thoroughly and for the sample to achieve equilibrium at 23°C and 50% RH.

Finally the tube is glued with epoxy glue to two aluminium ends which have a circular slot which fits exactly to the inner diameter of the tube.

Each tube is tested axially in a computer-controlled servo-hydraulic testing machine (MTS). The axial load is applied through universal joints and a roller bearing to obtain maximum freedom for rotation and bending of the ends. The internal pressure is applied through the lower end to a rubber bladder to maintain the humidity in the sample. When the bladder is blown up at the beginning of the loading, the air contained between the bladder and paper tube escapes through the paper.

The maximum load and maximum internal pressure for the specimens in this study are approximately 2 kN and 2 MPa respectively.

Using the computer to control it, the axial/radial stress ratio can be kept constant in each trial. This means that any biaxial combination of σ_1/σ_2 may be reached in a linear way in a given time. The time to failure in each trial is kept between 5 and 10 seconds. A computerised on-line graphical representation of σ_1 and σ_2 permits determination of whether or not axial compressional failure occurs before tensile radial failure.

The stress components in the axial (a) and radial (r) directions of a tubular specimen are easily computed from the axial force F, internal pressure P and radius a.

$$\sigma_a = P \cdot a \qquad \text{(force per unit width)} \qquad (15)$$

$$\sigma_r = F/2\pi a + Pa/2 \qquad \text{(force per unit width)} \qquad (16)$$

Evaluation of the shear strength S

In-plane shear strength evaluation by torsional testing of tubes made of thin sheets is very difficult due to the requirements of stability against buckling[8]. Normally, the shear stress σ_6 is computed from the torsional moment M by means of the following expression

$$\sigma_6 = M/2a^2\pi \qquad \text{(Force per unit width)} \qquad (17)$$

In the present investigation we had no access to equipment capable of subjecting the tubes to torsion. Instead, a 45^o off-axis specimen was used to evaluate the shear strength. This specimen was subjected to a stress ratio $\sigma_1/\sigma_2 = -1$, which is equivalent to pure shear loading in the principal material directions, as can be seen from the stress transformation equations in Table 1. The shear strength S is given by

$$S = |\sigma_{1F}| = |\sigma_{2F}| \tag{18}$$

where σ_{1F} and σ_{2F} are the stresses at failure in the 1- and 2-directions respectively.

3. Effects due to end constraints during load application

In order not to couple local material variations with the state of stress, the stresses in the sample should be both computable and uniform. For isotropic materials these requirements are easily met. For off-axis testing of orthotropic materials, deformation couplings can cause severe non-uniformity within the sample. Large errors may be introduced if the ends are rigid, because conventional clamping may introduce bending and shear when the specimen is subjected to tensile or compressive loading(21,22). A classic illustration of the effect of end-restraint on an off-angle straight specimen subjected to tensile loading is presented by Halpin et al.(22) in Figure 8.

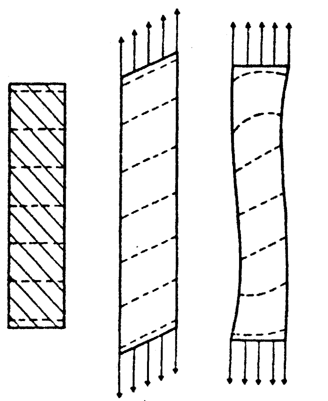

Fig 8—The effect of end-constraint on the deformation of 45° off-axis specimens. Source: Halpin, Pagano, Whitney and Wu (22).

The prevention of rotation or movement in off-axis specimens is equivalent to a superimposed shear stress for a given axial-radial stress ratio. The load is therefore applied to the paper tubes in figure 6 via universal joints mounted on a roller bearing.

4. Adhesive selection

Exploratory measurements were performed to find an adhesive with the following features to glue the two liner layers together:

1) Minimum penetration into the paper and avoidance of heat in order to retain the intrinsic paper structure.
2) Minimum strength increase.
3) High shear stiffness to provide a high resistance to buckling of the two layer composite, which is necessary to achieve adequate compression stability.
4) High bonding ability between the two layers.

A rubbery adhesive, PL400, manufactured by B.F. Goodrich was chosen as providing the best compromise between the desired features.

5. Flat specimen preparation and loading

Flat specimens were tested in the STFI solid support tester[6] shown in Figure 9 which permits pure compressional loading of the specimens.

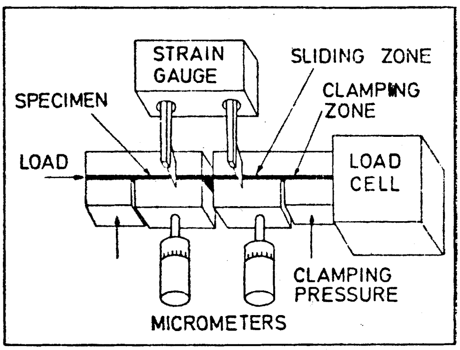

Fig 9—The STFI solid support tester. The specimen is prevented from buckling by steel blocks on each side of the specimen.

Flat two-layer specimens were manufactured and conditioned using the same technique as for the tubular specimens, except that they were not rolled up.

6. Evaluation of the testing procedure

The validity of using two-layer paper tubes for evaluating the general shape of the biaxial failure envelope was investigated. In particular, the effects of adhesive, buckling tendency and residual stresses were considered.

		1 Flat[1] one-layer	2 Flat[1] two-[3] layer	3 Tube[2] two-[3] layer	2/1 Diff %	3/2 Diff %	3/1 Diff %
Tensile Strength kN/m	MD	14.3	15.2	14.8(X)	+6	-3	+3
	CD	4.3	4.5	4.5(Y)	+5	+4	+4
Compression Strength kN/m	MD	4.7	5.4	4.6(X′)	+15	-15	-2
	CD	2.1	2.4	2.3(Y′)	+14	-4	+10
Elastic Modulus kN/m	MD	1730	1770		+2		
	CD	430	450		+5		
% Strain to failure in tension	MD	2.00	2.1		+5		
	CD	3.80	4.0		+5		
% Strain to failure in compression	MD	0.40	0.42		+5		
	CD	0.74	0.80		+8		

1) STFI solid support test. 2) MTS Materials testing system
3) Adhesive PL 400

Table 3

Strength data per layer of paper for the tested specimens made from 125 g/m^2 liner-board of 0.21 mm thickness. (Each value is the result of five tests.)

The effect of the adhesive is shown in a comparison between the two-layer and single-layer flat sheets in Table 3, column 2/1. It is evident that the adhesive has contributed moderately to the elastic modulus. However, it also appears that the high stretchability of the adhesive has resulted in better utilisation of the strain and strength potential of the sheets. The strength has increased 6-10% in tension and 14-15% in compression. The larger increase for compression is reasonable since the absolute strength of paper is lower in compression than in tension.

A study of the difference in strength between the flat and tubular two-layer specimens in Table 3, column 3/2, shows that whereas the tensile strength of the tubes is approximately equal to that of the flat sheets, the compression strength is 4-15 % lower for the tubes. This is attributed either to buckling on a small scale when the tubes are loaded in compression or to residual stresses in the radial direction which affect the compression strength in the axial direction. The same effects of specimen shape have earlier been reported(6) for single layer liner-board of grammages between 125-450 g/m^2.

The net effect due to the adhesive and specimen shape varies between -2 and +10% and is given in the final column of table 3.

In tension, the effect of residual stresses may be estimated by comparing the uniaxial tensile strengths of tubes with MD and CD in the axial and radial directions. The strength data in Table 4 show an insignificant difference between the two directions, which supports the assumption that residual stresses incorporated during manufacture have a minor effect on the strength properties in tension.

		Axial	Radial	Rad/Ax diff. %
Tensile	MD	14.8	13.8	-7
Strength kN/m	CD	4.5	4.7	+4

Table 4
Comparison of axial and radial tensile failures of two-layer tubes.
(Each point is the result of five tests.)

The results show a satisfactory consistency between the tubular and flat specimens, confirming that the buckling component is small and consequently that the paper may be considered to be loaded in pure compression. Furthermore, the influence of residual stresses on the tubes is small. The tubes are therefore considered to provide a valid technique for this investigation.

Experimental results

1. <u>On-axis biaxial loading</u>

From the results of the key tests presented in Table 3 the following four constants were calculated by means of equations (4) - (7).

$$F_{xx} = 0.015,\ F_x = -0.150,\ F_{yy} = 0.097,\ F_y = -0.213$$

Using an average biaxial strength of P = 6.2 kN/m, obtained by the application of an equal biaxial stress state and additional uniaxial strength values in Table 3, F_{xy} was determined from equation (8) to have the value

$$F_{xy} = -0.013$$

The shape of the failure envelope at zero shear stress is given in figure 10. The same figure shows also the best fit to equation (3) using the constants given above.

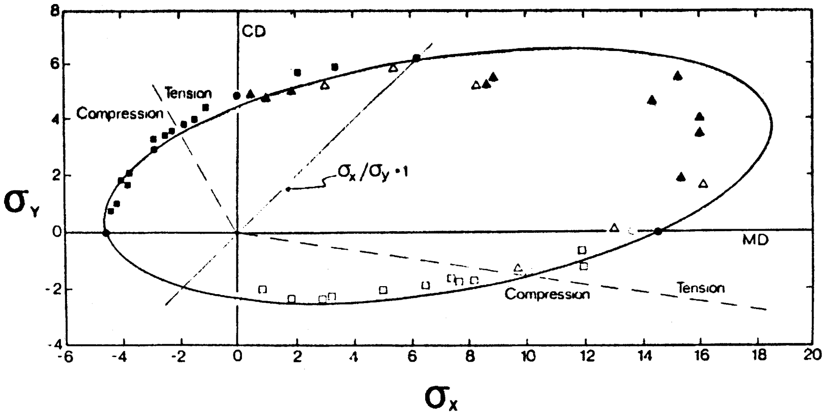

Fig 10—The shape of the failure envelope for on-axis tubular specimens. (The shear stress $\sigma_S = 0$.)

Key: MD axial: Key experiments ●
Mapping experiments, two-layer tube, diam. = 40 mm ■
One-layer tube, diam. = 80 mm ▲
CD axial: Key experiments ○
Mapping experiments, two-layer tube, diam. = 40 mm □
One-layer tube, diam. = 80 mm △

2. 45° off-axis biaxial loading

By subjecting a 45° off-axis specimen to an axial-radial stress ratio $\sigma_1/\sigma_2 = -1$ and loading it to failure, the shear strength S may be evaluated according to equation (18),

$$S = 3.1 \text{ kN/m}$$

The loading conditions and shear strength evaluation are illustrated in figure 11.

Using this value of the shear strength, F_{ss} may be evaluated according to equation (11):

$$F_{ss} = 0.104$$

Figure 11 shows the failure envelope for 45° off-axis tubular specimens, the Tsai-Wu equation (2) having been fitted to the experimental points. An excellent fit to the data is noted. Notice too that the points are symmetrical with respect to the line $\sigma_1 = \sigma_2$.

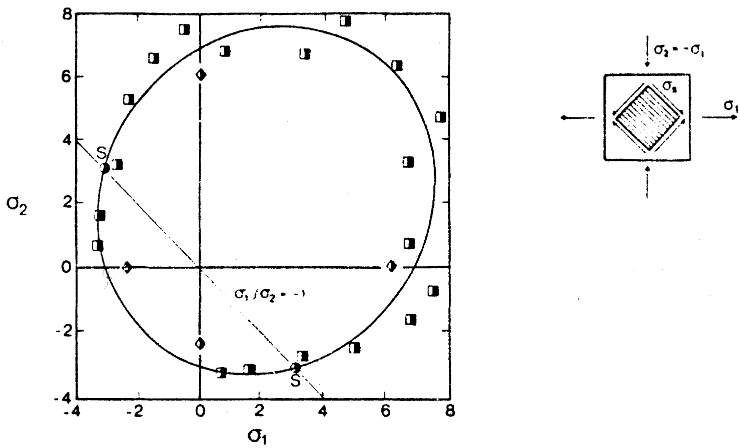

Fig 11—The shape of the failure envelope for 45° off-axis tubular specimens.
Key: Shear strength ○
Mapping experiments, two-layer tube □
Flat two-layer paper ◇

Figure 11 also shows uniaxial, off-axis data for the flat two-layer paper, where the ends are constrained through the use of the tester shown in Figure 9. The difference in strength between the tubular and flat specimens in tension and compression is indicated in Table 5. Compared with those given in Table 3, these differences indicate that there are larger differences between the two sample configurations when cut at 45° than when cut parallel to the machine axes. This is particularly true of compressive strength.

	1 Flat 1) one layer	2 Flat 1) two 3) layer	3 Tube 2) two 3) layer	2/1 Diff %	3/2 Diff %	3/1 Diff %
Tensile Strength kN/m	6.1	6.4	7.0 4)	+5	+9	+15
Compression Strength kN/m	2.3	2.6	3.0 4)	+13	+15	+30

1) STFI solid support test 2) MTS materials testing system
3) Adhesive PL 400 4) Interpolated value from figure 11

Table 5
Strength data per layer of paper for the tested 45° off-axis specimens. (Three tested for each result.)

Constrained ends lower the strength, as discussed in the experimental section: this is the explanation for the low strength of the flat two-layer paper. Thus it is not advisable to evaluate the strength of off-axis specimens if the specimen ends are constrained.

Simple way of determining the failure envelope for paper

The use of two-layer tubes is not suitable for routine purposes. Since the general shape of the failure envelope has been established for the liner-board paper investigated, and since it is reasonable to assume that the general shape does not vary for papers of different origin, only six key measurements are needed to establish the envelope shape. By introducing the following simplifications, the failure envelope may easily be established from simple uniaxial measurements.

a) Tensile and compressive strengths in the MD (X,X′) and CD (Y,Y′) are determined by uniaxial tensile and compressive tests on a flat paper strip, and the coefficients F_{xx}, F_x, F_{yy}, and F_y determined from equations (4) - (7).

b) The interaction term F_{xy} is determined from equation (9), assuming that the dimensionless coefficient F^*_{xy} = -0.36. This value was obtained in this study, and also for sack paper and envelope paper in a previous study[11].

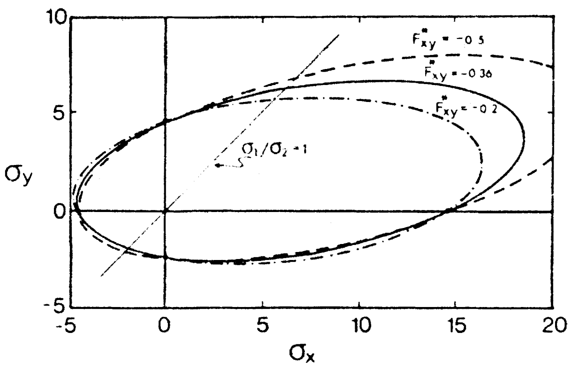

Fig 12—Sensitivity of the interaction term F^*_{xy} to the shape of the failure envelope.

The sensitivity to the interaction coefficient is shown in Figure 12 where the solid line represents a value of -0.36, the broken line a value of -0.5 (which is the value given by Tsai and Hahn[17] for the generalised von Mises criterion), and the dotted line a value of -0.20. It appears that the experimental results are best explained by a value of -0.36 or absolutely lower.

c) The shear strength of paper is the most difficult parameter to evaluate unambiguously. This subject has been treated by Setterholm et al.[8].

The shear strength S is evaluated by subjecting a 45° off-axis specimen to biaxial compression-tension load, and F_{ss} is determined by means of equation (11).

Shear failure always occurs in the compressive mode and the data in Figure 11 show that the numerical value of the shear strength S is therefore approximately equal to the uniaxial compression strength for the 45° specimen.

Furthermore the 45° compression strength is approximately equal to the geometric mean value of the uniaxial compression strengths in the MD and CD. The shear strength S then becomes:

$$S = \sqrt{X'Y'} \tag{19}$$

For the two-layer tubes S = 3.1 kN/m and $\sqrt{X'Y'}$ = 3.25kN/m, which means an error of less than 5%.

An approximate value of S may thus be obtained from the geometric mean of the MD and CD compression strengths.

Performance of liner-board in a corrugated container

1. Theoretical model

A mathematical model describing the stress situation in the liners due to internal pressure and top-to-bottom loading was proposed by Peterson and Fox[2-4]. In the model, the orthotropic material axes of the liners and corrugated medium coincide with the machine and cross-machine directions and the latter coincides with the vertical direction of the container.

Although paper shows strongly nonlinear stress-strain behaviour[5,6], the material is assumed to remain linear and elastic under load. The secant modulus in compression is used, determined as the slope of the line from the origin to the peak of the compression load in a stress-strain diagram. Interlaminar shear deformations are neglected.

According to Peterson and Fox(2-4), a simplified principal stress distribution in the inner liner of a corrugated container subjected to top to bottom loading may be computed.

In the panel centre region and at the panel boundaries a biaxial compressive stress state is predicted and in the corner regions a biaxial compression-tension stress state.

To determine in which part of the panel failure is most likely to occur, the biaxial stress state must be compared with a biaxial failure criterion.

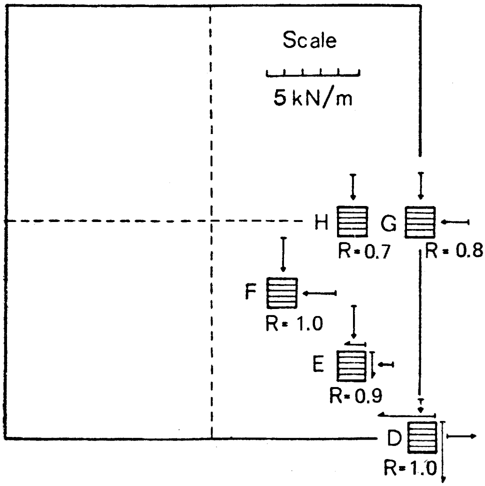

Fig 13—Corrugated container subjected to top-to-bottom loading. The magnitudes of the stresses are indicated by the lengths of the arrows. The stress state is related to the MD—CD axes. The safety factor R is given for each stress state. (CD coincides with the vertical direction of the container).

In the investigations by Peterson and Fox, no biaxial data were obtained and straight line segments in the failure envelope for normal stresses only (no shear) had to be assumed by analogy with the Tresca criterion shown in figure 1.

One of the main disadvantages of this criterion is that it follows no rules of transformation to other material directions. The failure envelope in all critical directions must be found experimentally or interpolated.

In the following paragraphs the use of the more appropriate Tsai-Wu tensor theory is demonstrated.

2. Application of the Tsai-Wu tensor theory to Safety factor evaluation

Using the Tsai-Wu tensor theory, the appropriate procedure is to transform any off-axis biaxial stress state to on-axis by means of Table 1, and then determine the safety factor by means of equation (14). The advantages of this approach are that all stresses are related to material properties in the orthotropic material directions, and that the effects of compression, tension, and shear may be separated.

Figure 13 shows the on-axis stress state in the inner liner of a corrugated container. This means that the principal stress state (shear stress = 0) proposed by Peterson and Fox is transformed to a more realistic state containing both normal and shear stresses.

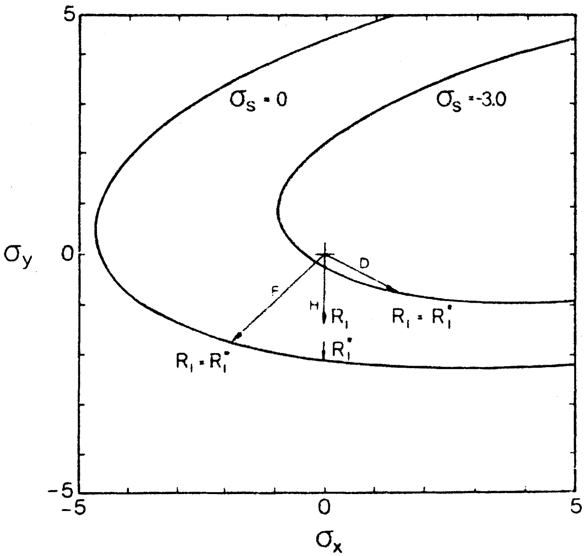

Fig 14—Graphical representation of the evaluation of the safety factor for points D, F and H in Fig 13. This part of Figs 4 and 10 represents the critical stress space where failure occurs.

No graphical representation of the failure criterion need be constructed, although this may aid in the assessment of the effects of changes in loading or material parameters. The visual representation of the safety factor $R = R_i/R_i^*$ is the relative length of a vector drawn from the stress state at a given point to the border of the failure envelope. The proper failure envelope for each point is given by the shear stress at that point. The higher the shear stress, the smaller is the envelope, as illustrated in Figure 14.

Figure 14 exemplifies the stress vectors for points D, F, and H in Figure 13. Point D has a safety factor R = 1 which means that the vector R_i has reached its failure envelope determined by the shear stress at the point. Points F and H include no shear component and have safety factors of 1 and 0.7 respectively.

Discussion

The present work has shown that the Tsai-Wu tensor theory is a workable tool to describe the biaxial failure envelope of paper. Measurements on paper have shown that it behaves not unlike other composite materials.

The experiments performed here have verified that under biaxial tension paper is considerably stronger than in uniaxial tension. These results qualitatively confirm those of a previous investigation[11] dealing with the biaxial tensile properties in the first quadrant. A qualitative explanation of the strength increase of paper in the biaxial tension mode is suggested in the work of van den Akker[25,26]. In uniaxial tension, compression forces develop in the fibre segments orientated within angles of $\pm 30^{\circ}$ to the transverse direction. These forces are subtracted from the theoretical sheet load, which is consequently numerically reduced. In the biaxial tension case, i.e. in the first quadrant, these forces change sign and become tensile, hence contributing to the theoretical sheet load. The same argument may be used to explain effects in at least the second and fourth quadrants as well.

In the third quadrant, biaxial compression, no results have yet been obtained. Thus it remains to be shown whether the mathematical expression of the envelope shape in this quadrant predicts physical reality.

Since failure in tension may be characterised by a disruptive cohesive failure, and failure in compression by a yielding type of failure, it is of fundamental interest to establish whether in the second and fourth quadrants there is any pronounced transitional region between tensile and compressional failure.

Figure 10 indicates the locations of the compression and tension regions of failure. It is concluded that within the limits of experimental precision, the experimental data show no discontinuity in the curves in the transition region between compressional and tensile failure.

In the proposed model for corrugated board failure, it is assumed that the liner-board remains flat up to the point of failure. In practice, liner-board does not always remain flat when loaded. On the contrary, several investigations predict interflute liner buckling[27,28]. Also for shear strength evaluation, Setterholm et al.[8] report difficulty in obtaining pure shear strength values due to buckling. The buckling tendency should diminish with increasing grammage.

The Tsai-Wu criterion outlined in this paper is a purely mathematical, phenomenological approach to materials testing and its application is not limited to simple stress-strain behaviour but also to more complex loading modes such as creep, fatigue and buckling. These buckling phenomena may therefore in principle be accounted for in the failure criterion. The failure criterion approach outlined in this paper should therefore be a universal tool in the paper industry for predicting the performance of products in complex loading situations.

Although it is recognised that corrugated boxes fail in a compressive mode[1-4] one of the controversies in the corrugated industry concerns the relative importances of the burst strength (Mullen) and the compression strength.

This question naturally has no simple answer, but it is safe to say that the tensile strength (burst) cannot be reduced to a value lower than the compressive strength. In such a case, the biaxial stresses on the outer liner of the container might reach critical values in a biaxial tensile mode, and such a mode of failure is obviously not acceptable with regard to protection of the contents of the box.

For the inner liner a lowering of the tensile strength would lead to a drastic change in the shape of the failure envelope and it is possible that the critical point of failure might switch from compression to tension, as illustrated in Figure 10.

A sufficient burst strength value may also be needed for other reasons, for instance in converting operations where scoring, cutting, and folding of the material demand high tensile strength values.

Acknowledgements

For skilful computer program design we thank Mr. Sune Karlsson. We also thank Mrs. Gunilla de Ruvo for experimental assistance and Mrs. Christina Benckert and Mrs. Inger Lindegren for typing the manuscript. For linguistic revision we thank Mr. Anthony Bristow.

REFERENCES

1. McKee, R.C., Gander, J.W., and Wachuta, J.R., Paperboard Packaging, 1963, **48**(8), p. 149-159.
2. Peterson, W.S., Tappi, 1980, **63**(10), 75-79.
3. Peterson, W.S., Tappi, 1980, **63**(11), 115-120.
4. Peterson, W.S. and Fox, T.S., Paperboard packaging, 1980, **65**(110), 68-76.
5. Cavlin, S. and Fellers, C., Svensk Papperstidn., 1975, **78**(9), 329-332.

6. Fellers, C., Paper Properties Compression. In. `Handbook of Physical and Mechanical Testing of Paper and Paperboard´ (Richard Mark, Ed.), Marcel Dekker, New York, in press.
7. `Bursting strength of Paper´ TAPPI, 1976, T 403 os-76.
8. Setterholm, V.C., Benson, R. and Kuenzi, E.W., Tappi, 1968, **51**(5), 196-202
9. Setterholm, V.C. and Gertjejansen, R.O., Tappi, 1965, **48**(5), 308-313.
10. Uesaka, T., Murakami, K. and Imamura, R., Tappi, 1979, **62**(8), 111-114.
11. de Ruvo, A., Carlsson, L. and Fellers, C., Tappi, 1980, **63**(5), 133-136.
12. Rowlands, R. E., ASME AMD Conference Proceedings, Nov. 30 - Dec. 5, 1975, Houston, Texas; p.97
13. Kaminski, B.E., and Lantz, R.B., Strength Theories of Failure of Anisotropic Materials, p. 160-169. In. `Composite Materials. Testing and Design´, ASTM STP 460, 1969.
14. Tsai, S.W., and Wu, E.M., J. Composite Materials, 1971, 5, p.58-80
15. Wu, E.M., J. Composite Materials, 1972, **6**, p.472-489
16. Wu, E.M., Phenomenological Anisotropic Failure Criterion, p.353-431, in. `Mechanics of Composite Materials´, (ed. G.I. Sendeckyj), Academic Press, New York, 1974
17. Tsai, S.W., and Hahn, H.T., `Introduction to Composite Materials´, Technomic Publishing Co., Inc., Westport, 1980
18. Jones, A. R., Tappi, 1968, **51**(5), 203-209.
19. Ashton, J.E., Halpin, J.C. and Petit, P.H., "Primer on Composite Materials. Analysis", Technomic Publications, Westport, Conn., 1969.
20. Timoshenko,, S., "Strength of Materials" Rober E. Krieger, New York, 1976
21. Pipes, R.B., J. Composite Materials, 1973, **7**, 246-252
22. Halpin, J.C., Pagano, N.J. Whitney, J.M. and Wu, E.M. Characterisation of Anisotropic Composite Materials, p. 37-47. In. "Composite Materials. Testing and Design., ASTM STP 460, 1969.

23. Timoshenko, S., Theory of Elastic Stability, 1936, McGraw Hill Book Co., inc., New York and London.
24. Carlsson, L., Fellers, C. and de Ruvo, A., J. of Materials Science, 1980, **15**, 2636-2642.
25. Van den Akker, J.A., personal communication.
26. Van den Akker, J.A., Tappi **53**(3).388 (1970).
27. Johnson, M.W., Urbanik, T.J., and Denniston, W.E., Paperboard and Packaging, 1980, **65**(4), 98-108.
28. Moody, R.C., U.S. Forest Service Research Paper FPL 46, 1965

Transcription of Discussion

Discussion following papers given by Prof. R.W. Perkins, and by Dr. C. Fellers.

Prof. J. Silvy, Ecole Francaise de Papeterie

Firstly, in the example given of the length distribution, was the sample beaten?

Secondly, how long does it take to obtain the information from a complete run in your process?

Prof. R.W. Perkins, Syracuse University, USA

I don´t think the pulp was beaten, but I am not certain because it comes ready prepared from STFI. I do know that it was a bleached softwood kraft.

Our procedure is quite rapid, because although the digitising must be done manually, to do it the cursor need only be placed on each individual point. No intermediate stopping or steps are necessary. The total time for a run involves the manufacture and digitising, and this was done for all 600 fibres per sample.

Prof. J. Silvy

As a point of information, it takes us an hour and a half to digitise 1800 fibres at Grenoble.